Light Sheet Fluorescence Microscopy using Incoherent Light Detection

Mariana Potcoava[1]

Christopher Mann[2,3], Jonathan Art[1], Simon Alford[1]

[1]Department of Anatomy and Cell Biology, University of Illinois at Chicago, 808 South Wood Street, Chicago, IL 60612, USA
[2] Northern Arizona University, Department of Applied Physics and Materials Science, Flagstaff, AZ, U.S.A, 86011
[3] Northern Arizona University, Center for Materials Interfaces in Research and Development, Flagstaff, AZ, U.S.A, 86011

Holography meets Advanced Manufacturing, 20-22 February 2023

THE UNIVERSITY OF ILLINOIS COLLEGE OF MEDICINE

DEPARTMENT OF ANATOMY AND CELL BIOLOGY

NAU NORTHERN ARIZONA UNIVERSITY

Outline

- Light-Sheet and Lattice Light-Sheet (LLS) Microscopy
- Incoherent Holography Lattice Light-Sheet System (IHLLS) with high NA (HNA) and low NA (LNA)
- Results
  - LLS and IHLLS 1L Beads Volume Reconstruction
  - IHLLS 2L Beads Volume Reconstruction
  - System Performances in LLS, IHLLS 1L, and IHLLS 2L
  - Neuronal Cells Imaging using IHLLS 2L
- Conclusion

Light-Sheet (LS) systems

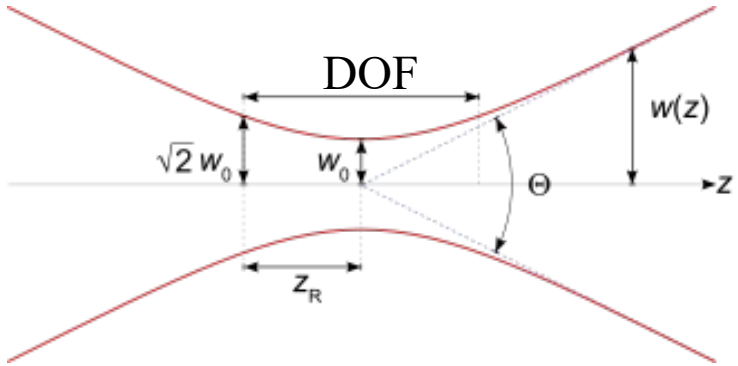

The excitation plane is created by using a cylindrical lens to shape the Gaussian laser beam in a sheet of light.

Strengths:

1. Optical sectioning
2. Extremely fast, no need for point scanning
3. Low phototoxicity/photobleaching

Weakness:

Tradeoff between the size of the beam (light sheet waist (w0) or light sheet thickness and the depth of field (DOF) or the light sheet length) and the axial resolution.

Conclusion: thin and long light sheet cannot be created with a Gaussian intensity profile laser beam !

https://en.wikipedia.org/wiki/Light_sheet_fluorescence_microscopy

Lattice Light-Sheet (LLS)

B.-C. Chen, et all, "Lattice light-sheet microscopy: Imaging molecules to embryos at high spatiotemporal resolution," Science 346, 1257998 (2014).

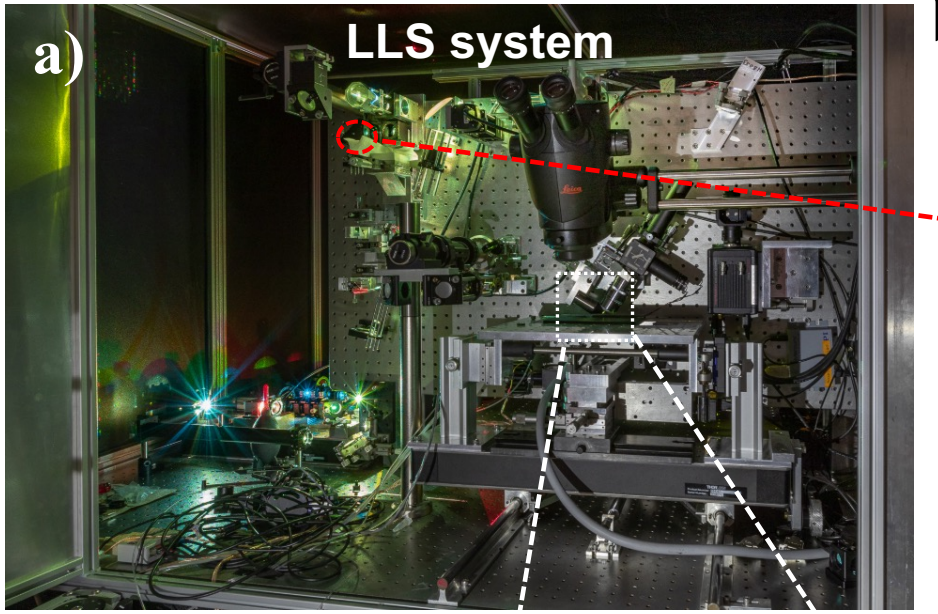

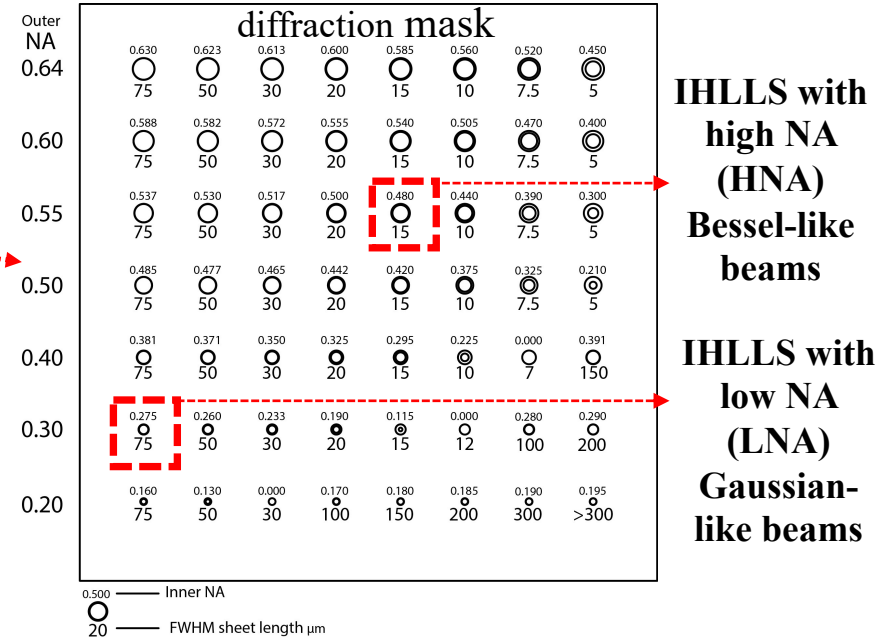

$$w_{sheet} = \lambda_{excitation}/2\,NA_{out}$$

$$\text{length}_{\text{sheet}} = \frac{\lambda_{escitation}}{n(cos\theta_{in} - cos\theta_{out})}$$

$$\theta_{in} = arsin(NA_{in}/n)$$

$$\theta_{out} = arsin(NA_{out}/n)$$

Gao, L. Optimization of the excitation light sheet in selective plane illumination microscopy. Biomed. Opt. Express 2015, 6, 881-890, doi:10.1364/BOE.6.000881.

Weakness:

3D scanning by moving the detection objective or the sample stage!

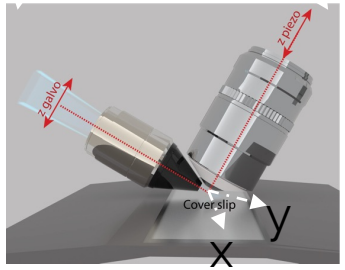

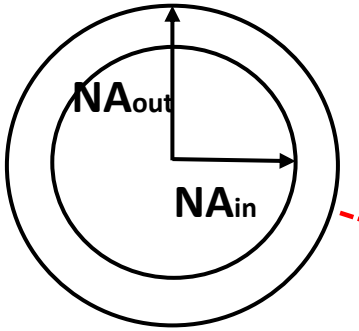

Annular filter at the excitation pupil

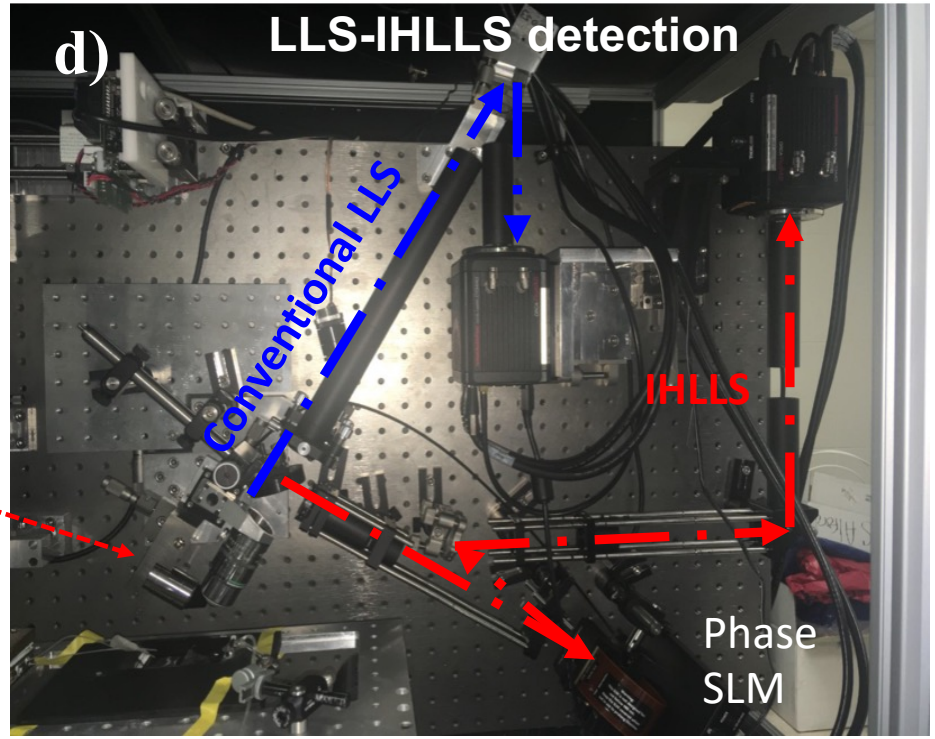

IHLLS System using FINCH

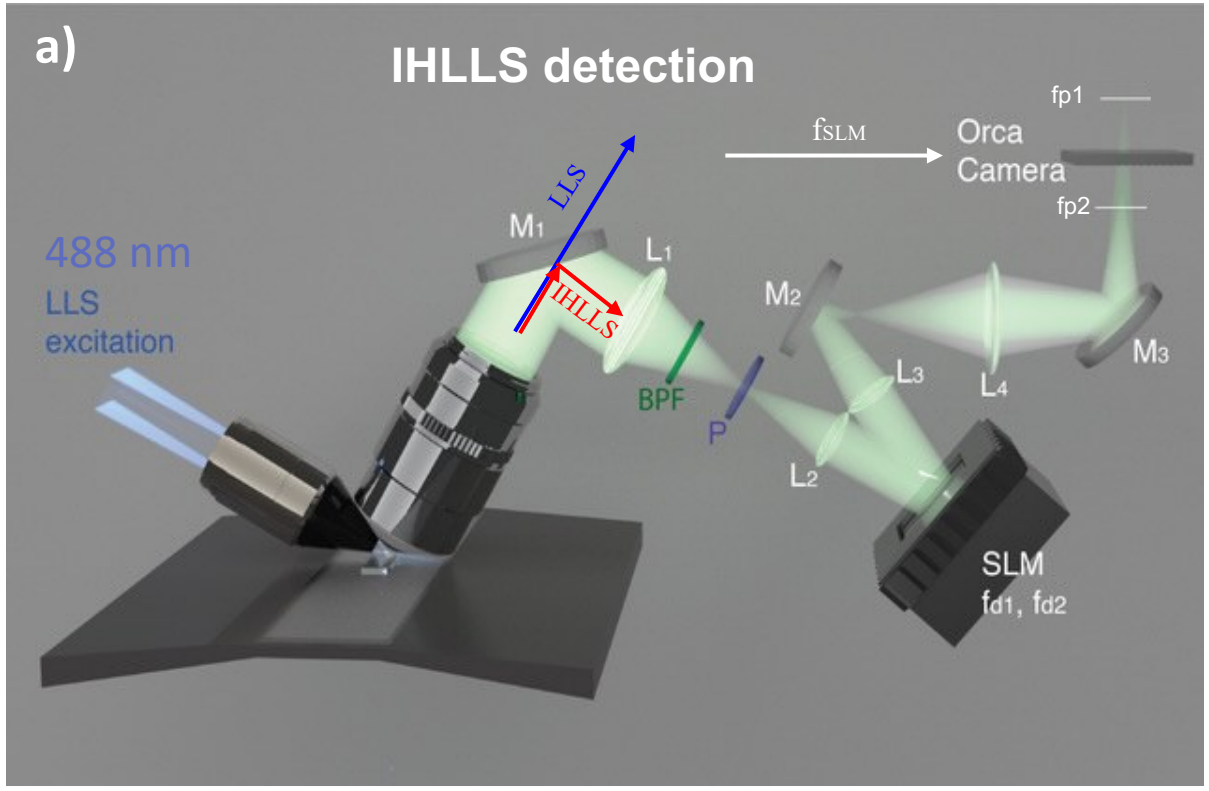

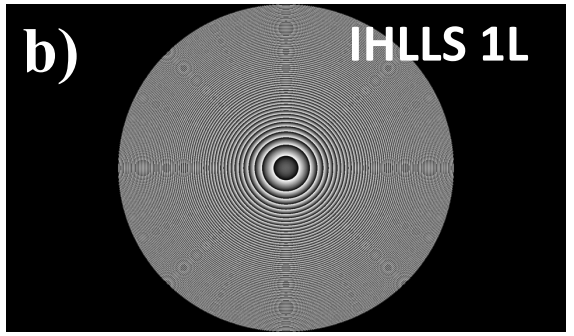

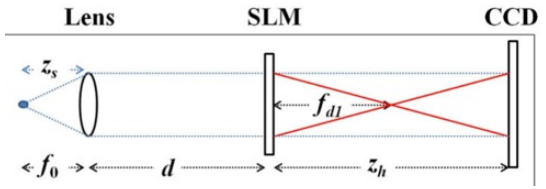

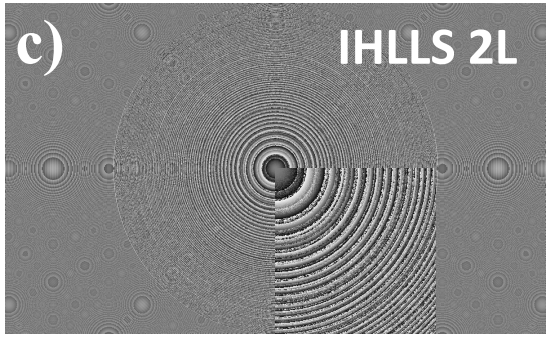

J. Rosen, et all, "Theoretical and experimental demonstration of resolution beyond the Rayleigh limit by FINCH fluorescence microscopic imaging," Opt Express **19**, 26249-26268 (2011).

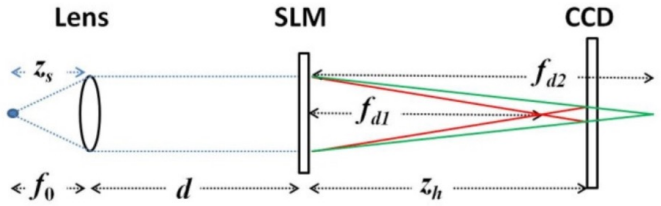

LLS

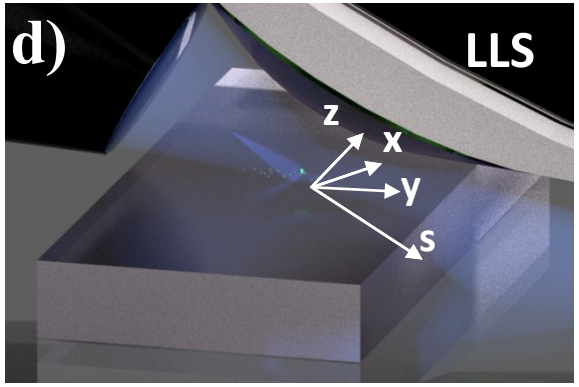

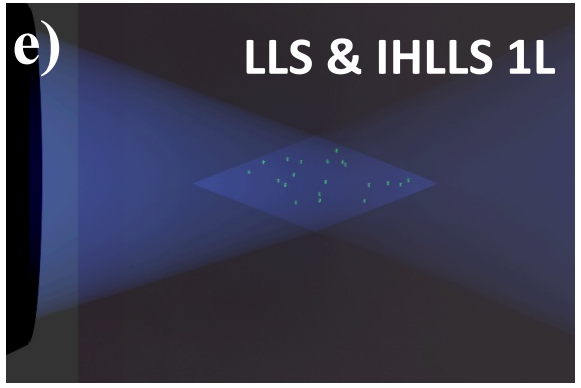

IHLLS

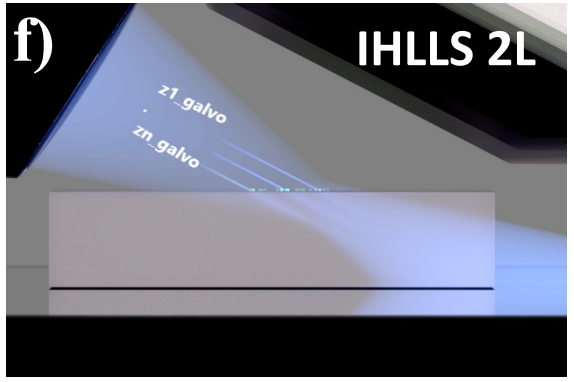

Excitation and Scanning Geometry in LLS, IHLLS Systems

Special Optics 0.65 NA

25x Nikon 1.1 NA

a)

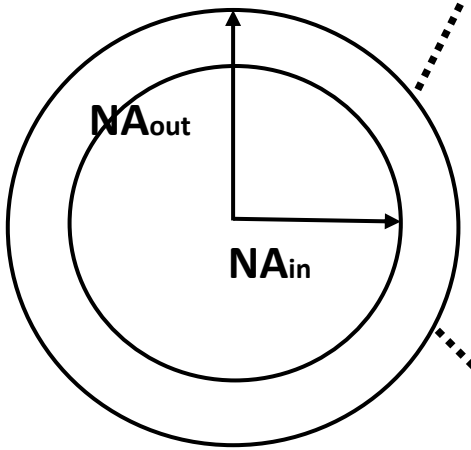

Annular filter at the excitation pupil

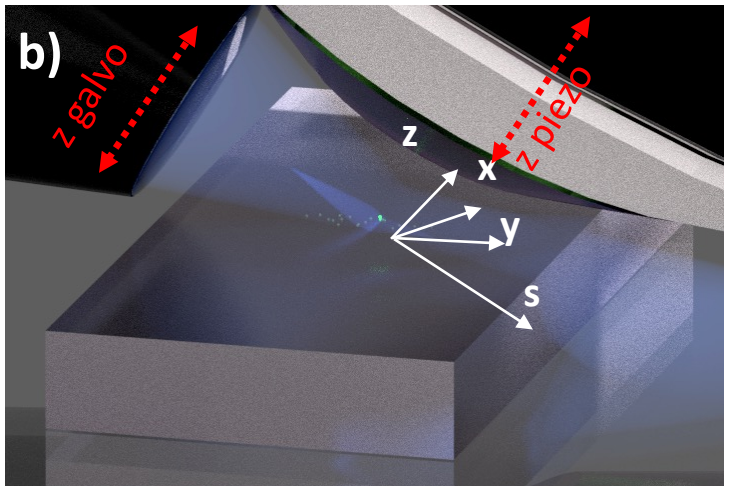

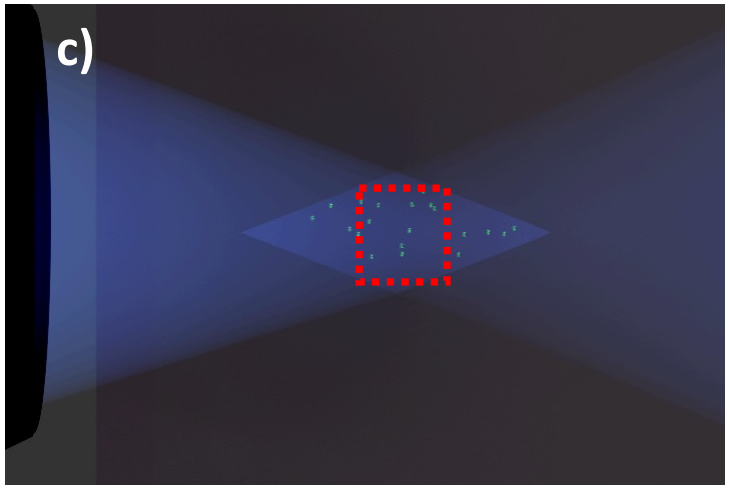

LLS, IHLLS 1L

IHLLS 2L

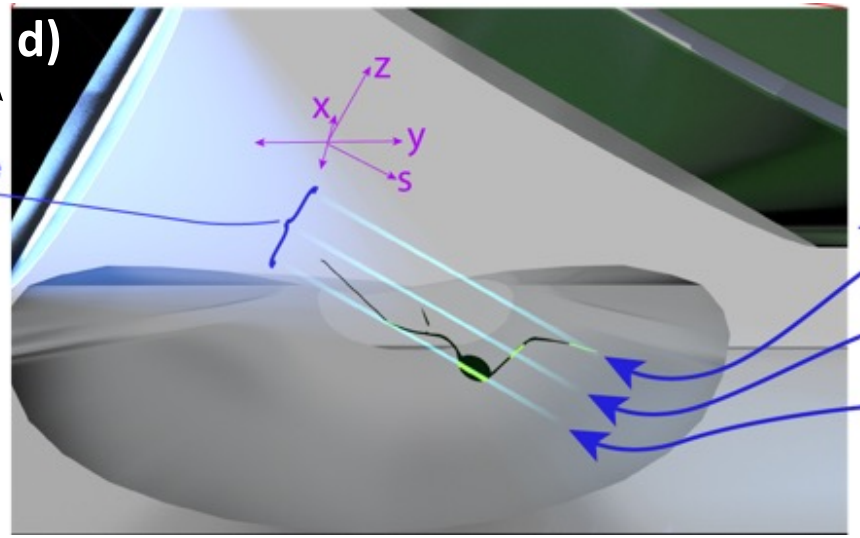

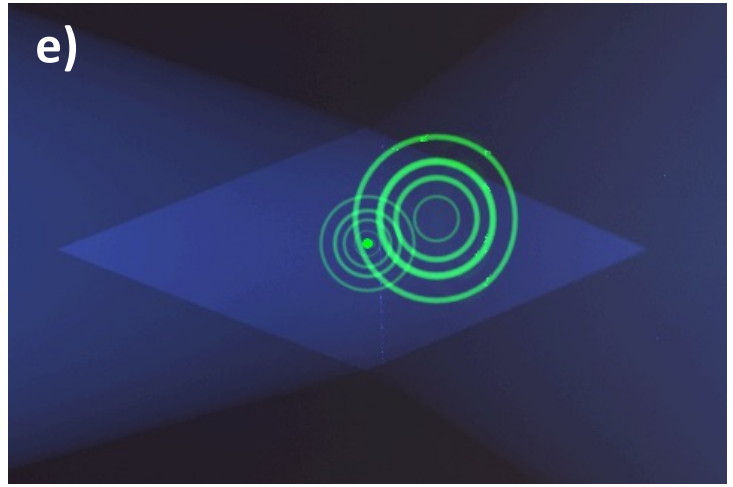

Optical Lattices Generation using HNA and LNA Annuli

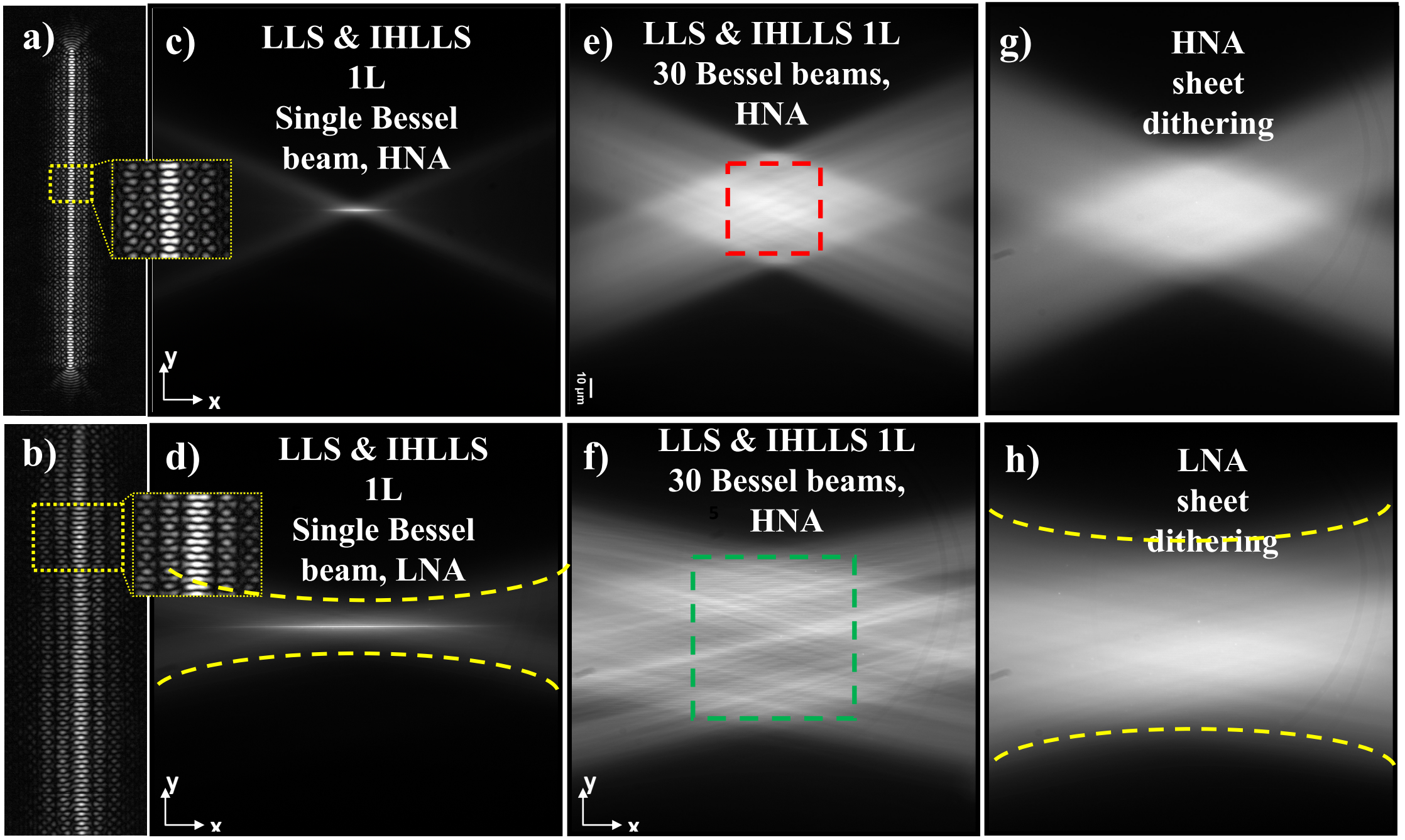

LLS and IHLLS 1L Beads Volume Imaging

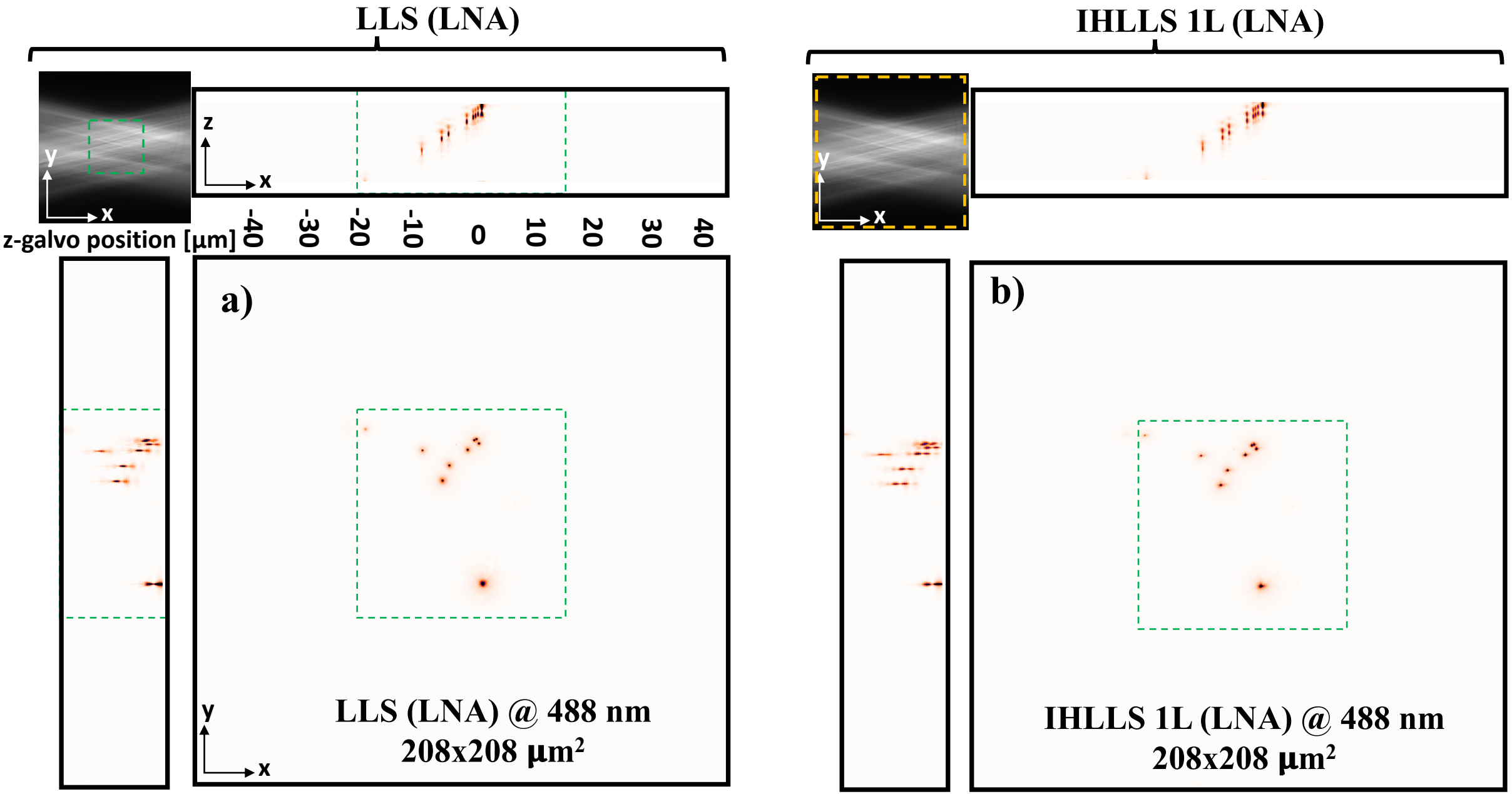

IHLLS 2L (LNA) Beads Holography

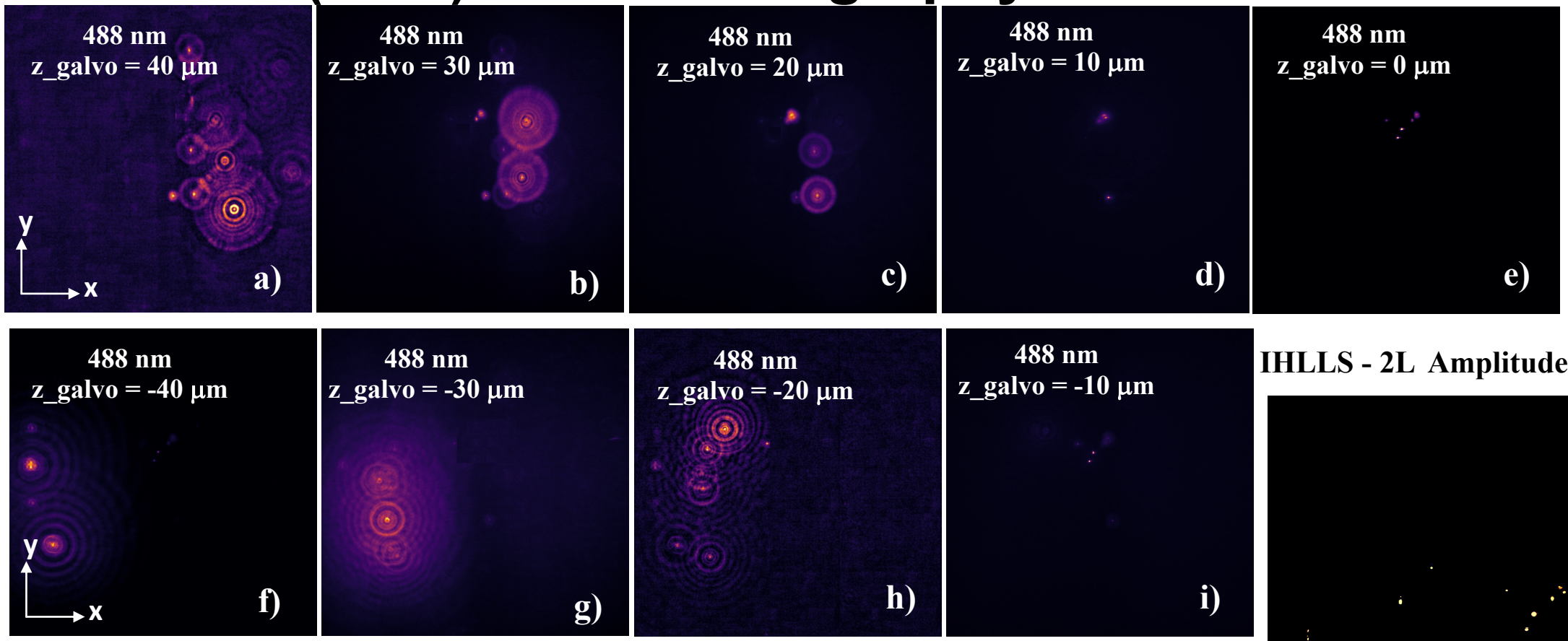

IHLLS 2L (LNA) Intensity Images at θ = 0

IHLLS - 2L Amplitude Reconstruction

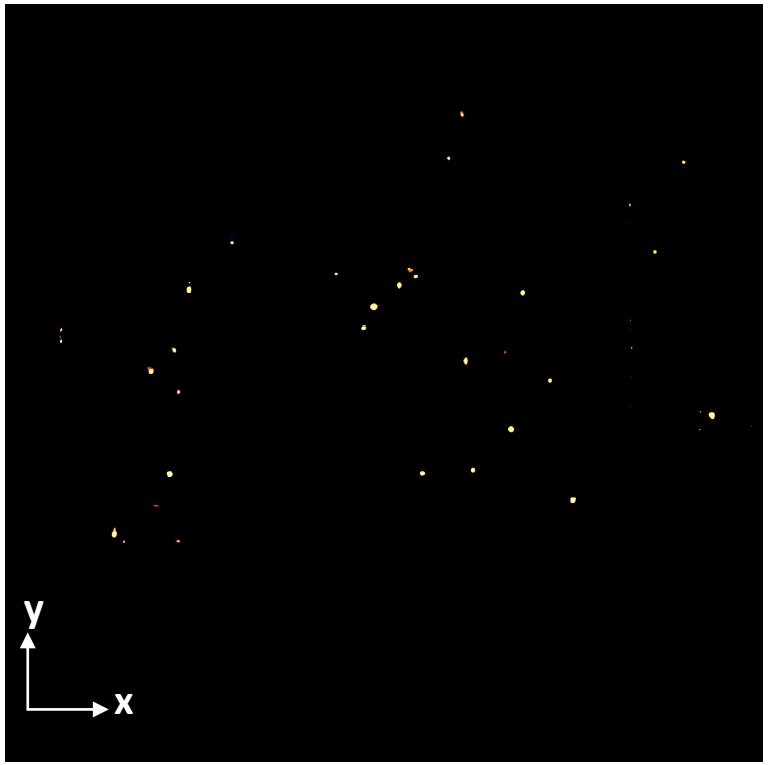

IHLLS 2L (LNA)
@ 488 nm
208x208 μm²

Imaging Comparison Between IHLLS 2L and LLS

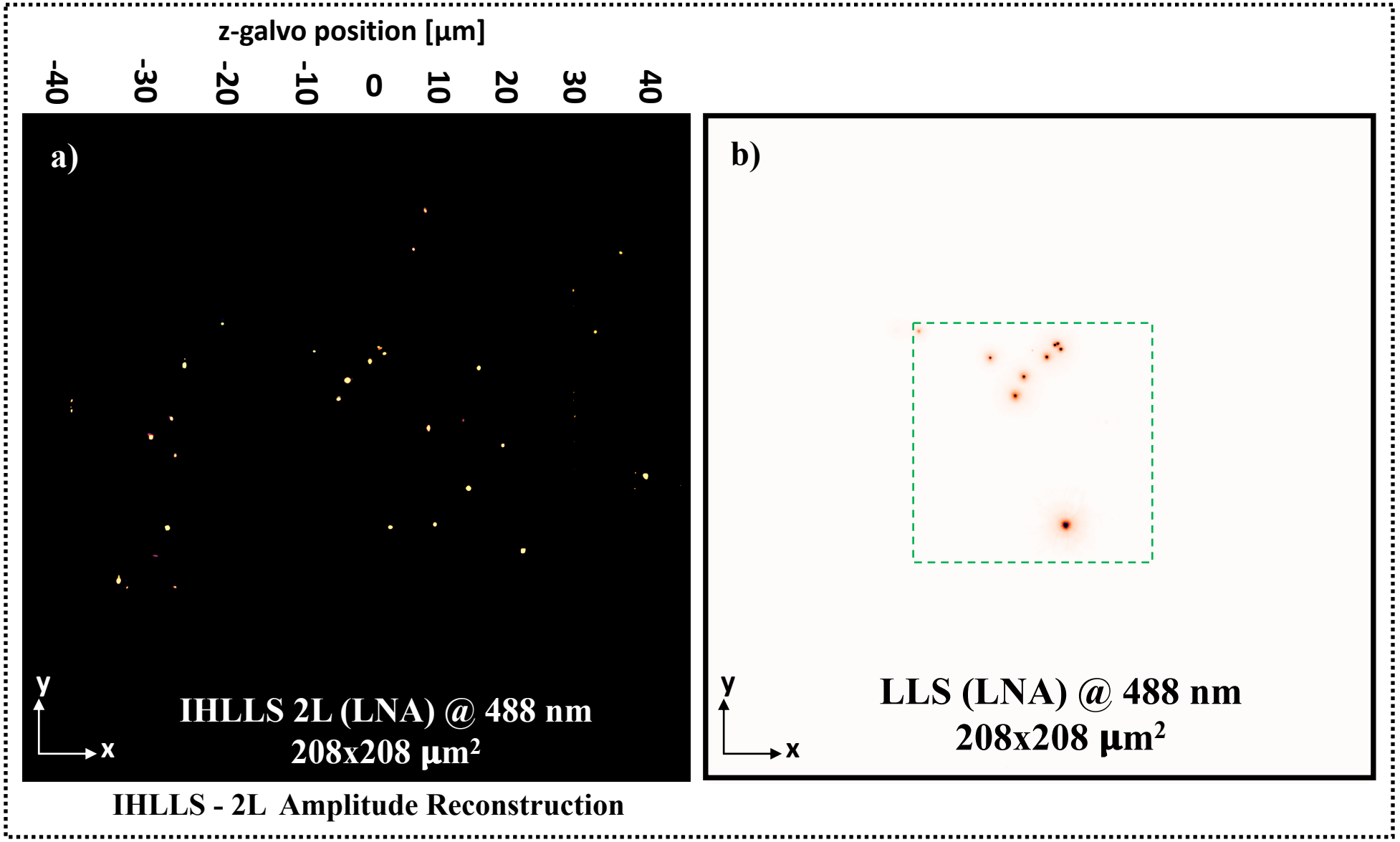

IHLLS - 2L Amplitude Reconstruction

ICHLLS (HNA, 488 nm & 561 nm) Colocalization

Colocalization of two dyes was measured by labeling a lamprey motoneuron with 10,000 MW dextran conjugated to Alexa 555 and Alexa 488 applied 24 hours prior to the experiment by injection into the myotomal muscles.

Imaging was then performed using:

- ICHLLS -1L with 400 z-axis planes in the range -30 μm to 30 μm in 10 μm steps exciting sequentially with 488 nm (a) and 561 nm (b) light;
- ICHLLS -2L reconstructed amplitude images (e, f) and phase images (I, j) with 9 z-axis planes in the range -40 μm to 40 μm in 10 μm steps, exciting sequentially with 488 nm and 561 nm light;

The colocalization maps (c, g, k) and the scatter plot (d, h, l) for each case are displaced on the right.

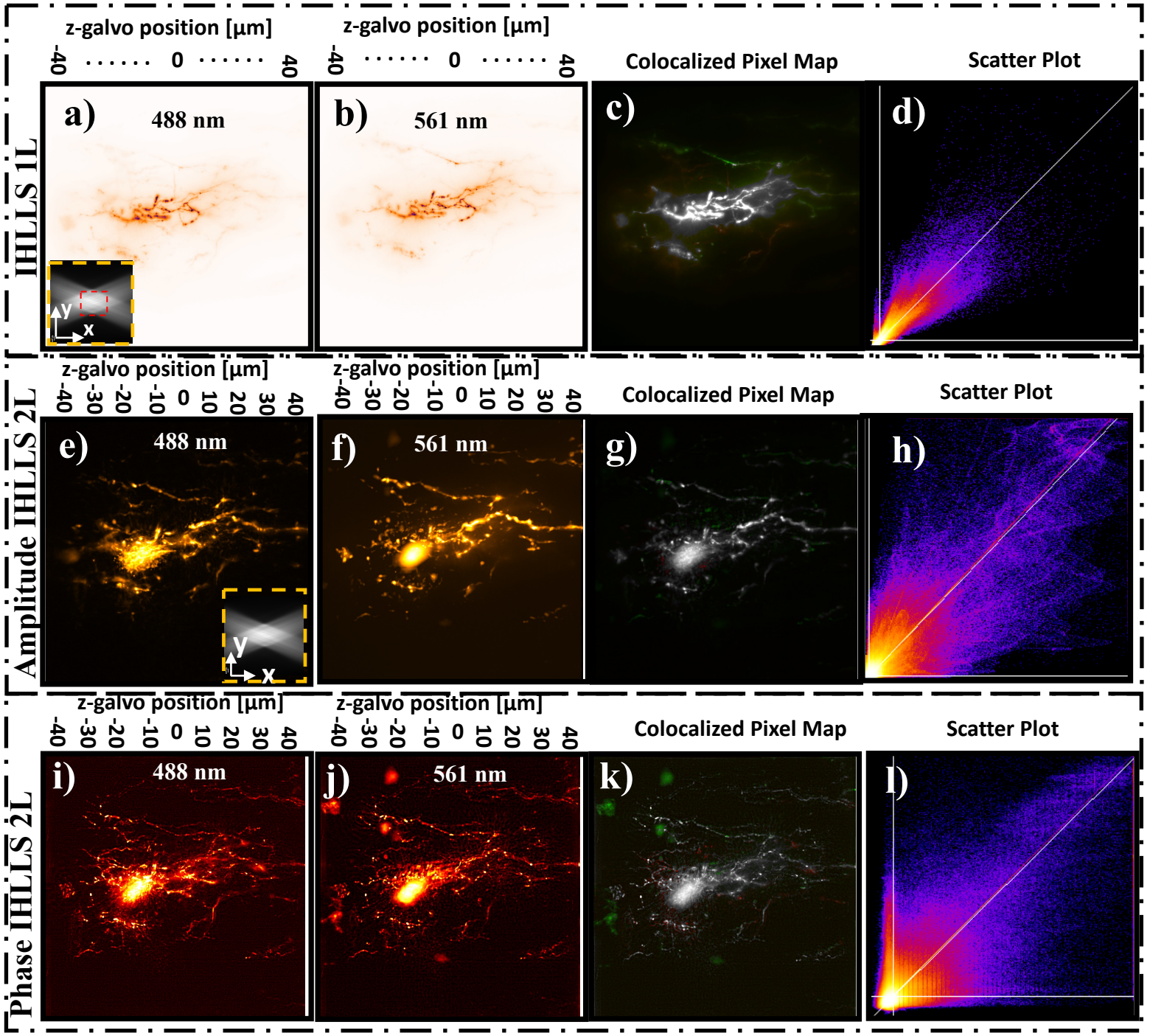

Deformation Measurements of Neuronal Excitability using LLS and IHLLS (HNA, 488 nm)

LLS and ICHLLS 1L imaging

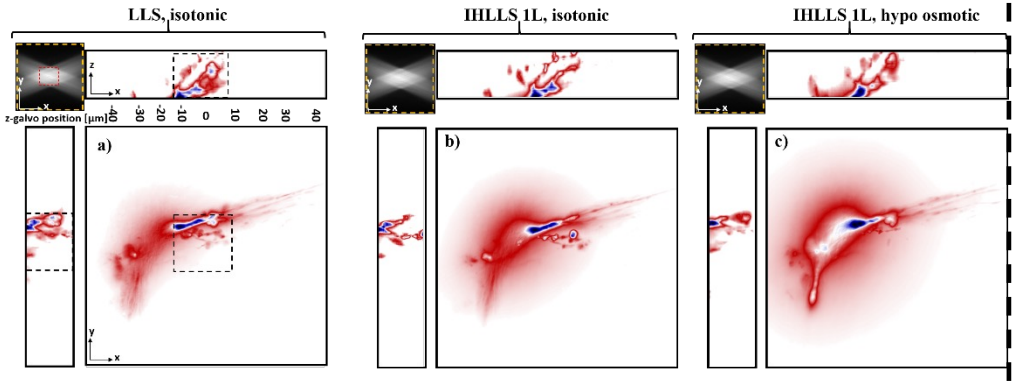

Tomographic imaging of a lamprey spinal cord ventral horn neuron with dendrites, xy FOV 208 x 208 µm², yz, (xz) FOV 208 x 40 µm², in a conventional LLS **(a)** and incoherent LLS with only one diffractive lens (ICHLLS 1L, 488 nm) of focal length 400 mm.

ICHLLS 2L , 488 nm, imaging of a lamprey spinal cord ventral horn neuron with dendrites in a Ringer's solution (a-i) and hypotonic solution (j-s);

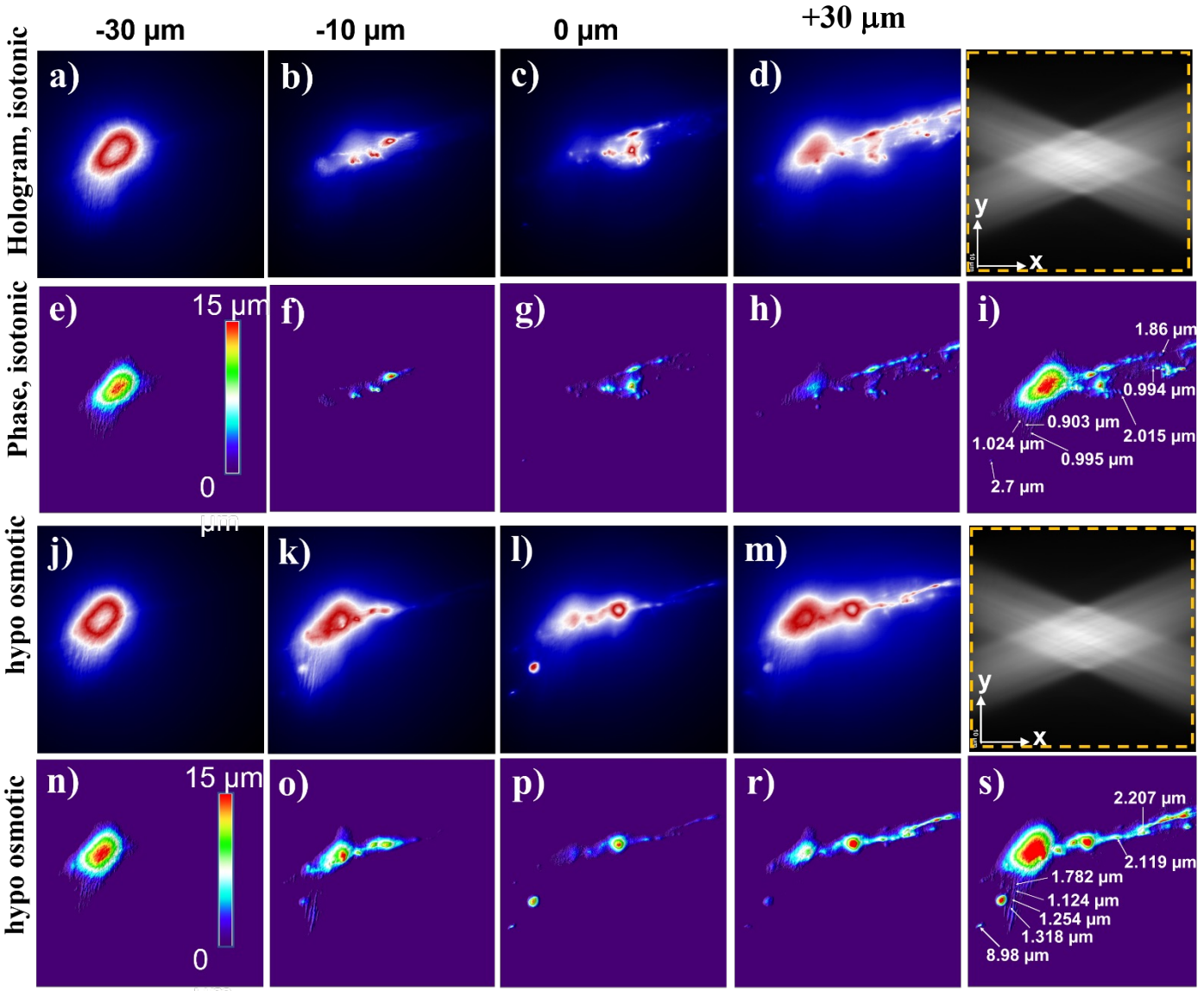

LLS and IHLLS (HNA, 488 nm) Imaging of a Lamprey Spinal Cord Ventral Horn Neuron with Dendrites

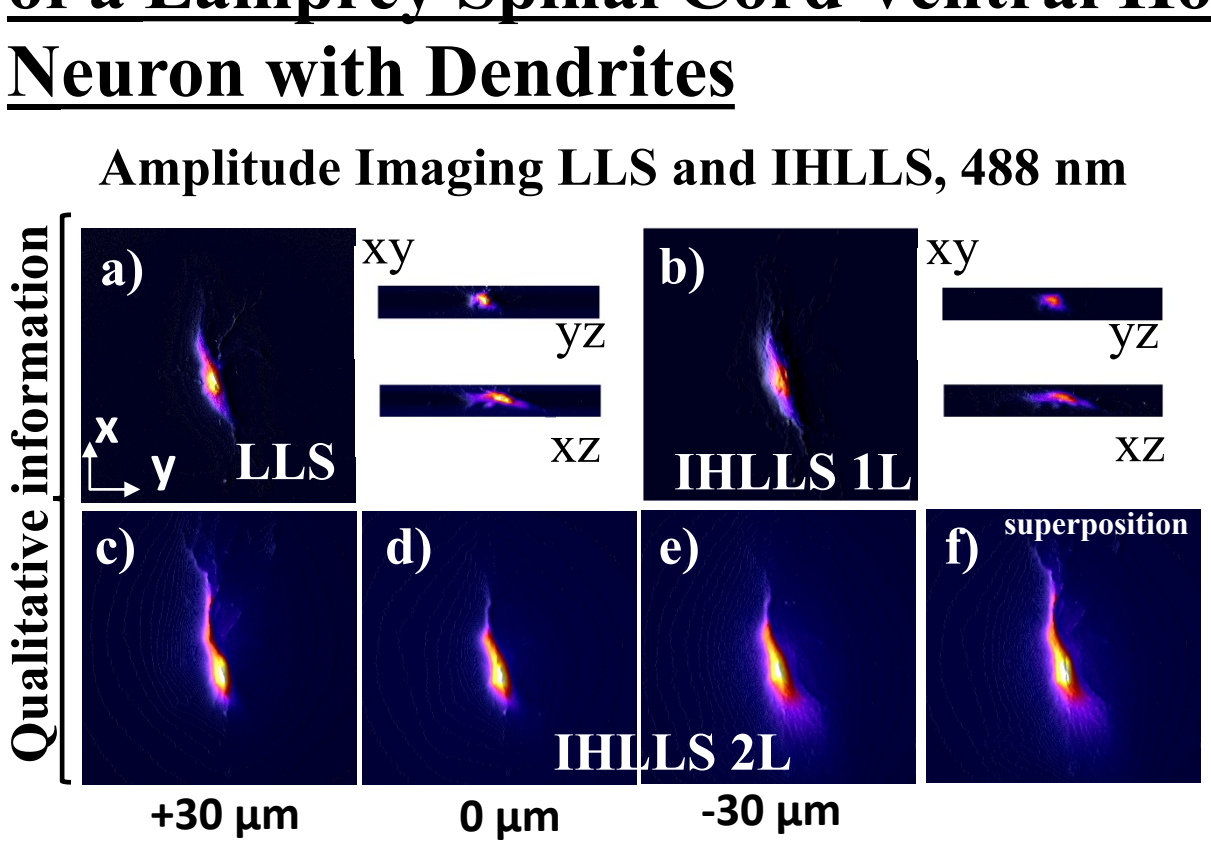

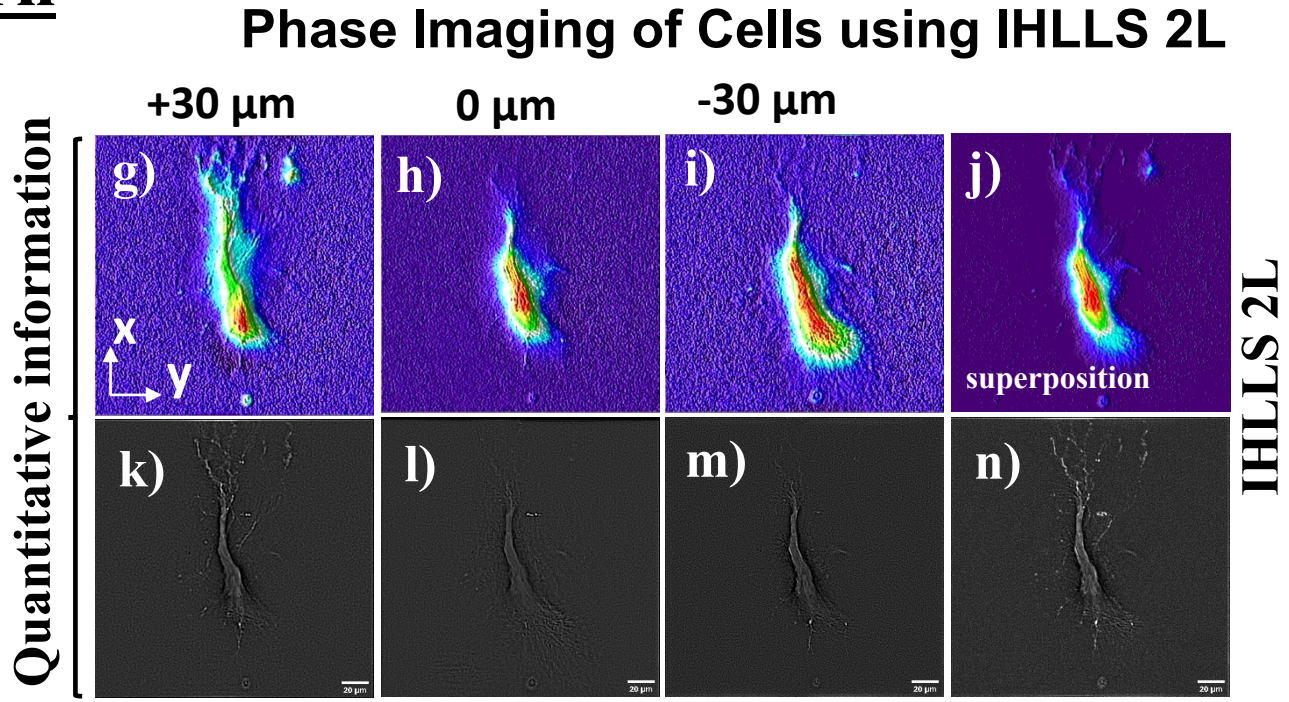

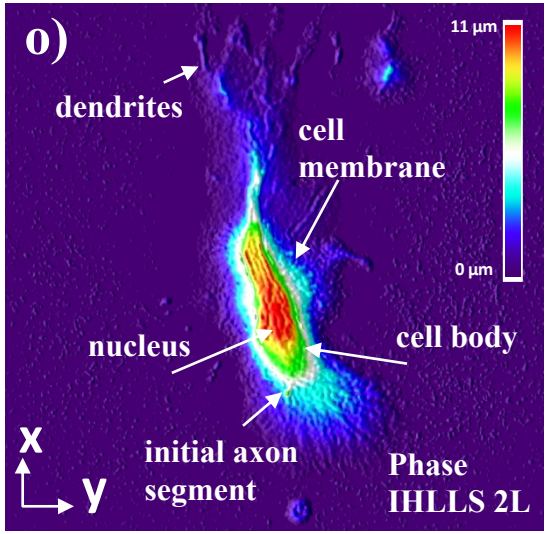

a) Max projections through the volume (300 z-galvo and z-piezo steps) in a conventional LLS system without deconvolution; **b)** Max projections through the volume (300 z-galvo and z-piezo steps) using IHLLS 1L without deconvolution; Amplitude reconstruction of a neuronal cell using ICHLLS 2L, 488 nm, at three z-galvo positions: **c)** +30µm, **d)** 0µm, **e)** -30µm, and **f)** the superposition of all three; Phase reconstruction of a neuronal cell at z-galvo positions: **g)** +30µm, **h)** 0µm, **i)** -30µm, and **j), o)** the superposition of all three; **k)-n)** Band-pass filter applied to the phase images from **g)-j).**

SUMMARY

- We showed IHLLS imaging using longer and lower resolution beams.
- The IHLLS approach to generate holograms to resolve 3D positional information is functional.
- Maximum detector FOV of $208 \text{ x } 208\ \mu m^2$.
- IHLLS-2L provides a better method for finding the focal position of the objects than using analog glass optics.
- Performed 3D imaging without moving the sample stage or the detection objective.
- Because the objective position is fixed, images at the center of the z galvo range are brighter, therefore we modulated the laser power and exposure time in the z axis.

Thank You

Alford, S.; Mann, C.; Art, J.; Potcoava, M. Incoherent color holography lattice light-sheet for subcellular imaging of dynamic structures. *Frontiers in Photonics* 2023, *4*, 1096294, doi:10.3389/fphot.2023.1096294.

Potcoava M, Mann C, Art J, Alford S. Extended Lattice Light-Sheet with Incoherent Holography. In: Rosen J, editor. Holography - Recent Advances and Applications [Internet]London: IntechOpen; 2022. Chapter 12; Available from: DOI: 10.5772/intechopen.107322.

Mariana Potcoava, Christopher Mann, Jonathan Art, and Simon Alford, "Spatio-temporal performance in an incoherent holography lattice light-sheet microscope (IHLLS)," Opt. Express 29, 23888-23901 (2021).

Potcoava M, Art J, Alford S, Mann C. Deformation Measurements of Neuronal Excitability Using Incoherent Holography Lattice Light-Sheet Microscopy (IHLLS). *Photonics*. 2021; 8(9):383.

Rosen, J.; Alford, S.; Anand, V.; Art, J.; Bouchal, P.; Bouchal, Z.; Erdenebat, M.-U.; Huang, L.; Ishii, A.; Juodkazis, S.; Kim, N.; Kner, P.; Koujin, T.; Kozawa, Y.; Liang, D.; Liu, J.; Mann, C.; Marar, A.; Matsuda, A.; Nobukawa, T.; Nomura, T.; Oi, R.; Potcoava, M.; Tahara, T.; Thanh, B.L.; Zhou, H. Roadmap on Recent Progress in FINCH Technology. *J. Imaging* 2021, *7*, 197.

Simon Alford (UIC)

Jonathan Art (UIC)

Christopher Mann (NAU)

Acknowledgement: This work was supported by grants NIH RO1 NS111749 and NIH R21 DC017292.